

# Gravitational waveforms and radiation powers of the triple system PSR J0337+1715 in modified theories of gravity

Xiang Zhao<sup>1,2</sup>, Chao Zhang<sup>1,2</sup>, Kai Lin<sup>3,4</sup>, Tan Liu<sup>5,6</sup>, Rui Niu<sup>5,6</sup>, Bin Wang<sup>7,8</sup>,  
Shaojun Zhang<sup>2</sup>, Xing Zhang<sup>5,6</sup>, Wen Zhao<sup>5,6</sup>, Tao Zhu<sup>2</sup>, and Anzhong Wang<sup>1,2\*†</sup>

<sup>1</sup> GCAP-CASPER, Physics Department, Baylor University, Waco, TX 76798-7316, USA

<sup>2</sup> Institute for Theoretical Physics & Cosmology,

Zhejiang University of Technology, Hangzhou 310032, China

<sup>3</sup> Hubei Subsurface Multi-scale Imaging Key Laboratory, Institute of Geophysics and Geomatics,  
China University of Geosciences, Wuhan, Hubei, 430074, China

<sup>4</sup> Escola de Engenharia de Lorena, Universidade de São Paulo, 12602-810, Lorena, SP, Brazil

<sup>5</sup> CAS Key Laboratory for Researches in Galaxies and Cosmology, Department of Astronomy,  
University of Science and Technology of China, Chinese Academy of Sciences, Hefei, Anhui 230026, China

<sup>6</sup> School of Astronomy and Space Science, University of Science and Technology of China, Hefei 230026, China

<sup>7</sup> Center for Gravitation and Cosmology, Yangzhou University, Yangzhou 225009, China and

<sup>8</sup> School of Physics and Astronomy, Shanghai Jiao Tong University, Shanghai 200240, China

(Dated: July 19, 2022)

In this paper, we study the gravitational waveforms, polarizations and radiation powers of the first relativistic triple systems PSR J0337 + 1715, observed in 2014, by using the post-Newtonian approximations to their lowest order. Although they cannot be observed either by current or next generation of the detectors, they do provide useful information to test different theories of gravity. In particular, we carry out the studies in three different theories, general relativity (GR), Brans-Dicke (BD) gravity, and Einstein-aether ( $\mathfrak{a}$ ) theory. The tensor modes  $h_+$  and  $h_\times$  exist in all three theories and have almost equal amplitudes. Their frequencies are all peaked at two locations,  $f_1^{(+,\times)} \simeq 0.0686656\mu\text{Hz}$  and  $f_2^{(+,\times)} \simeq 14.2138\mu\text{Hz}$ , which are about twice of the outer and inner orbital frequencies of the triple system, as predicted in GR. In  $\mathfrak{a}$ -theory, all the six polarization modes are different from zero, but the breathing  $h_b$  and longitudinal  $h_L$  modes are not independent and also peaked at two frequencies. A somehow surprising result is that these peaked frequencies are not two times of those of the inner and outer orbital frequencies, as for the  $h_+$  and  $h_\times$  modes, but instead, they are almost equal to them,  $f_1^{(b,L,\mathfrak{a})} \simeq 0.0457771\mu\text{Hz}$  and  $f_2^{(b,L,\mathfrak{a})} \simeq 7.09545\mu\text{Hz}$ . A similar phenomenon is also observed in BD gravity, in which only the three modes  $h_+$ ,  $h_\times$  and  $h_b$  exist, where  $f_1^{(b,BD)} \simeq f_1^{(b,L,\mathfrak{a})}$  and  $f_2^{(b,BD)} \simeq f_2^{(b,L,\mathfrak{a})}$ . We also study the radiation powers, and find that the quadrupole emission in each of the three theories has almost the same amplitude, but the dipole emission can be as big as the quadrupole emission in  $\mathfrak{a}$ -theory. This can provide a very promising window to obtain severe constraints on  $\mathfrak{a}$ -theory by the multi-band gravitational wave astronomy.

## I. INTRODUCTION

The concept of gravitational waves (GWs) was first developed by Einstein in 1916 right following his general theory of relativity (GR). He proposed that GWs are the ripples of spacetimes that are propagating with the speed of light [1]. A century passed, the Laser Interferometer Gravitational-Wave Observatory (LIGO) first verified his GW theory by directly detecting the GW signal on Sep. 14, 2015 [2]. After this, ten more GWs have been detected by LIGO Scientific Collaboration and Virgo Collaboration [3–8]. The sources of these eleven GW events were all from binary systems of black holes, except for the signal GW170817, which was from a binary neutron stars [7].

In fact, there are about 13% of low-mass stellar systems containing three or more stars [9], and 96% of low-mass

binaries with periods shorter than 3 days which are part of a larger hierarchy [10]. Recently, a realistic triple system was observed, named as PSR J0337 + 1715 (J0337 for short) [11], which consists of an inner binary and a third companion. The inner binary consists of a pulsar with mass  $m_1 = 1.44M_\odot$  and a white dwarf (WD) with mass  $m_2 = 0.20M_\odot$  in a 1.6 day orbit. The outer binary consists of the inner binary and a second dwarf with mass  $m_3 = 0.41M_\odot$  in a 327 day orbit. The two orbits are very circular with its eccentricities  $e_I \simeq 6.9 \times 10^{-4}$  for the inner binary and  $e_O \simeq 3.5 \times 10^{-2}$  for the outer orbit. The two orbital planes are remarkably coplanar with an inclination  $\lesssim 0.01^\circ$  [See Fig. 1].

A triple system is an ideal place to test the strong equivalence principle [12]. Remarkably, after 6-year observations, recently it was found that the accelerations of the pulsar and its nearby white-dwarf companion differ fractionally by no more than  $2.6 \times 10^{-6}$  [13], which provides the most severe constraint on the violation of the strong equivalence principle.

In this paper, we investigate this triple system in three different theories of gravity, GR, Brans-Dicke (BD) grav-

\*Corresponding Author

†Electronic address: Anzhong.Wang@baylor.edu

ity, and Einstein-aether ( $\mathfrak{a}$ ) theory, by using the post-Newtonian approximations to their lowest order. We shall pay particular attention on the differences predicted by these theories. Although neither the current generation of detectors nor the next one can detect the GWs emitted by this system, it serves well as a realistic example to show clearly the different predictions from each of these theories. In particular, we shall study the radiation power, gravitational waveforms, their polarizations, and Discrete Fourier transform (DFT). Among the modified theories of gravity,  $\mathfrak{a}$ -theory locally breaks the Lorentz symmetry by introducing a globally time-like unit vector field (the  $\mathfrak{a}$ ther) [14], while in BD gravity the gravitational interaction is mediated by both a scalar and a tensor fields [15].

Specifically, the paper is organized as follows: In Sec. II, we study the gravitational waveforms, polarization modes and their Fourier transforms in GR, BD gravity and  $\mathfrak{a}$ -theory, respectively, while in Sec. III we investigate the emission powers of the GW in each of these three theories. Due to the presence of the extra vector and scalar modes in  $\mathfrak{a}$ -theory, and only the scalar mode in BD gravity, the total emission power is different in each of the three theories. In particular, we find that the dipole emission in  $\mathfrak{a}$ -theory can be as large as the quadrupole emission in GR, which can provide a very promising window to obtain severe constraints on  $\mathfrak{a}$ -theory by the multi-band gravitational wave astronomy [16]. There also exists an appendix, in which we present a very brief introduction to  $\mathfrak{a}$ -theory [14].

In this paper, we will adopt the following conventions: All the repeated indices  $i, j, k, l$  ( $i, j, k, l = 1, 2, 3$ ) will be summed over regardless they are up or down, while repeated indices  $a, b, c$  ( $a, b, c = 1, 2, 3$ ) will not be summed over unless the summation is explicitly indicated. We also set the speed of light equal to one ( $c = 1$ ). The metric signature is  $(-, +, +, +)$ .

## II. GRAVITATIONAL WAVEFORMS AND THEIR POLARIZATIONS

When a GW passes two test masses, the distance between them will be changed. Assuming that  $\zeta^i$  denotes the spatial coordinates between these two test masses in the Minkowski coordinates  $x^\mu = (t, x, y, z)$ , the equations of the geodesic deviation in the weak-field approximations read,

$$\ddot{\zeta}_i = -R_{0i0j}\zeta^j, \quad (2.1)$$

where  $i, j = 1, 2, 3$ , as mentioned previously, and  $R_{\mu\nu\alpha\beta}$  denotes the linearized Riemann tensor, which is determined by the field equations of a given theory. Different theories will have different field equations, so different theories also yield different components of  $R_{0i0j}$ . Therefore, in the following we shall consider the three theories, GR, BD gravity, and  $\mathfrak{a}$ -theory, separately.

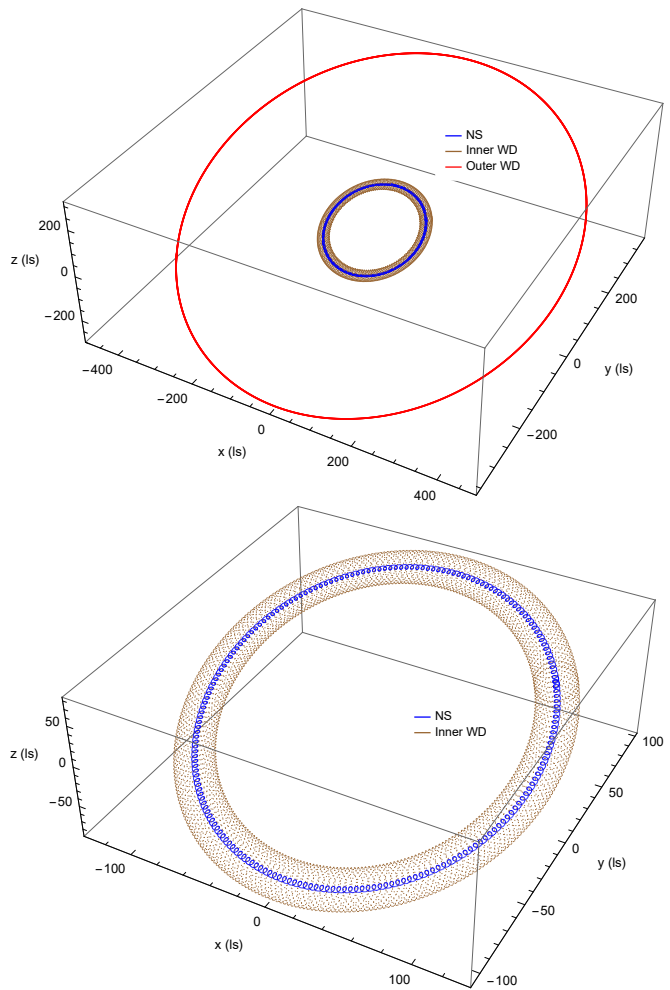


FIG. 1: Orbit of the NS, inner WD and the outer WD where ls stands for the light second. This plot shows the trajectories observed in the center-of-mass system for about 330 days starting from 01-04-2012 [12]. Note that to save memory, instead of plotting the trajectories over 500 days, here we just plot it for 330 days.

### A. Gravitational Waveforms and Their Polarizations in GR

In GR, the equations of the geodesic deviation take the form [17],

$$\ddot{\zeta}_i = -R_{0i0j}\zeta^j = \frac{1}{2}\ddot{h}_{ij}^{TT}\zeta^j, \quad (2.2)$$

where

$$h_{ij}^{TT}(t, \mathbf{x}) = \frac{2G_N}{R}\ddot{Q}_{ij}^{TT}(t - R), \quad (2.3)$$

with  $R \equiv |\mathbf{x}|$  denoting the distance from the observer to the source and  $G_N$  denoting the Newtonian constant. In the above equations,  $TT$  represents the transverse-traceless part of the tensor, which can be obtained by

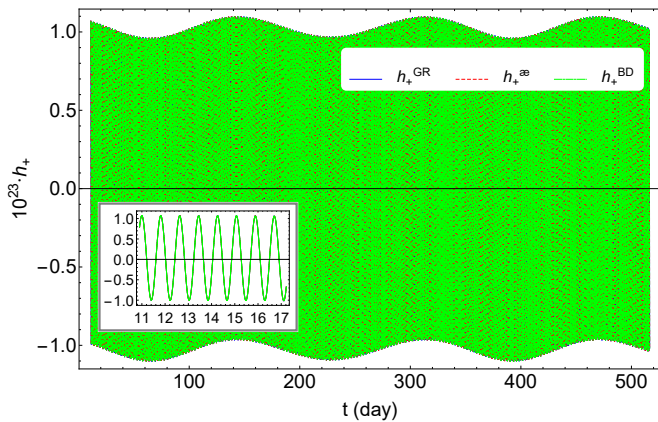


FIG. 2: The plus polarization  $h_+$ , respectively, in GR, æ-theory and BD gravity for about 500 days with an inserted plot for about 7 days. Note that the amplitudes are amplified by a factor  $10^{23}$ .

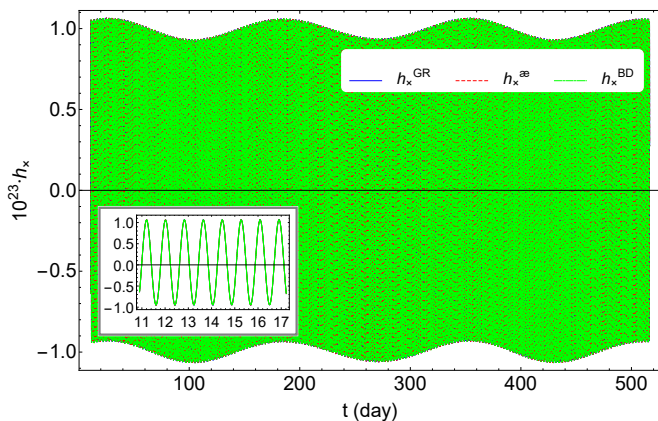


FIG. 3: The cross polarization  $h_\times$ , respectively, in GR, æ-theory and BD gravity for about 500 days with an inserted plot for about 7 days. Note that the amplitudes are amplified by a factor  $10^{23}$ .

applying  $TT$  operator  $\Lambda_{ijkl}$ ,

$$\Lambda_{ijkl}(\mathbf{N}) = P_{ik}P_{jl} - \frac{1}{2}P_{ij}P_{kl}, \quad (2.4)$$

where  $P_{ij}(\mathbf{N}) = \delta_{ij} - N_i N_j$ . Let's introduce a set of orthogonal bases,  $(\mathbf{e}_X, \mathbf{e}_Y, \mathbf{e}_Z)$ , where  $\mathbf{e}_Z \equiv \mathbf{N}$  denotes the propagation direction of the GW from the source to the observers. Thus,  $(\mathbf{e}_X, \mathbf{e}_Y)$  forms a plane orthogonal to the propagation direction  $\mathbf{N}$  of the GW. In the  $(t, x, y, z)$  coordinates, they are given by,

$$\begin{aligned} \mathbf{e}_X &= (\cos \vartheta \cos \varphi, \cos \vartheta \sin \varphi, -\sin \vartheta), \\ \mathbf{e}_Y &= (-\sin \varphi, \cos \varphi, 0), \\ \mathbf{e}_Z &= (\sin \vartheta \cos \varphi, \sin \vartheta \sin \varphi, \cos \vartheta), \end{aligned} \quad (2.5)$$

where  $\vartheta$  and  $\varphi$  are the two spherical angular coordinates. For the case of J0337,  $\vartheta$  and  $\varphi$  are  $0^\circ$  and  $270^\circ$ , respectively [11]. In GR,  $h_{ij}^{TT}$  has only two degrees of freedom,

and corresponds, respectively, to the plus (“+”) and cross (“ $\times$ ”) polarizations, which are given by,

$$h_+^{GR} = \frac{G_N}{R} \ddot{Q}_{kl} e_+^{kl}, \quad h_\times^{GR} = \frac{G_N}{R} \ddot{Q}_{kl} e_\times^{kl}, \quad (2.6)$$

where  $e_+^{kl} \equiv e_X^k e_X^l - e_Y^k e_Y^l$ ,  $e_\times^{kl} \equiv e_X^k e_Y^l + e_Y^k e_X^l$ . In Figs. 2 and 3, we plot these two components, from which it can be seen that the amplitudes of both modes is about  $10^{-23}$ , which is in the range of the designed sensitivity of the current generation of the ground-based detectors, such as, LIGO, Virgo and KGRA, but not their frequencies (See, e.g. [18]).

To obtain the Fourier transform for each polarization mode, instead of using the continuous Fourier transform,  $\tilde{h}_A(f) = (2\pi)^{-1} \int h_A(t) e^{-i2\pi f t} dt$ , we adopt the discrete Fourier transform (DFT),

$$\tilde{h}_A(f_n) \equiv \frac{1}{N} \sum_{k=0}^{N-1} h_A^k e^{-i2\pi n k / N}, \quad (2.7)$$

where  $h_A^k \equiv h_A(t_k)$ ,  $t_k = \Delta k$ , where  $\Delta$  is a real constant, and  $N$  and  $n$  are integers. Clearly, once  $\Delta$ ,  $N$  and  $n$  are chosen,  $\tilde{h}_A(n)$  is uniquely determined. In this paper, we shall use the built-in values of Mathematica. With this in mind, in Figs. 4 and 5 we plot  $\tilde{h}_+(f)$  and  $\tilde{h}_\times(f)$ , respectively, where  $f = \{f_0, f_1, \dots, f_{N-1}\}$  with  $f_n \equiv n/(N\Delta)$ . In these figures, it can be seen clearly that there are two peaks at the locations,

$$\begin{aligned} f_{\text{outer}}^{(+,\times)} &\simeq 0.0686656 \mu\text{Hz} \simeq 2.00102 \times f_{\text{outer}}^{\text{orb}}, \\ f_{\text{inner}}^{(+,\times)} &\simeq 14.2138 \mu\text{Hz} \simeq 1.94152 \times f_{\text{inner}}^{\text{orb}}, \end{aligned} \quad (2.8)$$

where the outer and inner orbital frequencies  $f_{\text{inner}}^{\text{orb}}$  and  $f_{\text{outer}}^{\text{orb}}$  of the triple system are given by,

$$f_{\text{inner}}^{\text{orb}} \simeq 7.10327 \mu\text{Hz}, \quad f_{\text{outer}}^{\text{orb}} \simeq 0.0353669 \mu\text{Hz}. \quad (2.9)$$

Thus,  $f_{\text{outer}}^{(+,\times)}$  and  $f_{\text{inner}}^{(+,\times)}$  are about twice of the outer and inner orbital frequencies of the triple system, but not exactly equal. In GR, for a binary system the GW frequency is exactly equal to two times of their orbital frequency [17]. However, it must be noted that here the difference is due to the presence of the third component of the triple system.

## B. Gravitational Waveforms and Their Polarizations in æ-Theory

In æ-theory, the equation of the geodesic deviation reads [19],

$$\ddot{\zeta}_i = -R_{0i0j} \zeta^j \equiv \frac{1}{2} \ddot{P}_{ij} \zeta^j, \quad (2.10)$$

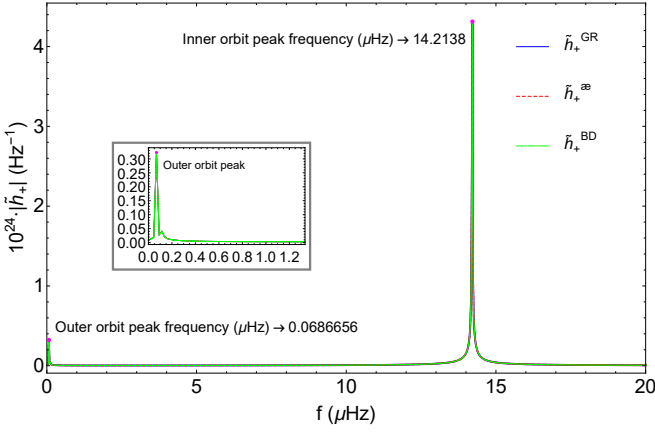


FIG. 4: DFT of the plus polarization  $\tilde{h}_+(f)$ , respectively, in GR,  $\text{ae}$ -theory and BD gravity, where the two peaked frequencies have been marked. Note that the amplitudes are amplified by a factor  $10^{24}$ .

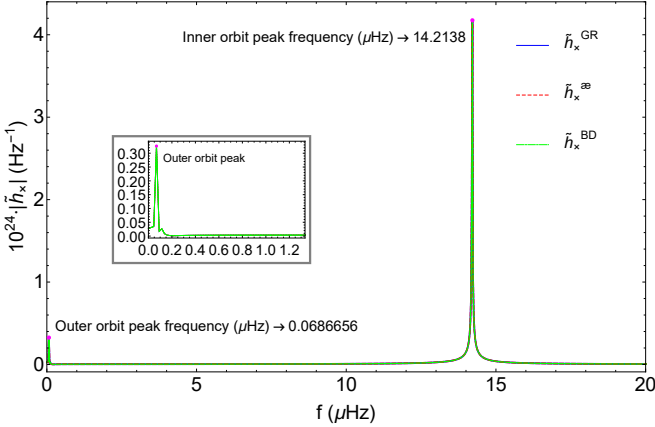


FIG. 5: DFT of the cross polarization  $\tilde{h}_\times(f)$ , respectively, in GR,  $\text{ae}$ -theory and BD gravity, where the two peaked frequencies have been marked. Note that the amplitudes are amplified by a factor  $10^{24}$ .

where

$$\mathcal{P}_{ij} = \phi_{ij} - \frac{2c_{13}}{(1-c_{13})c_V} \Psi^I_{(i} N_{j)} - \frac{c_{14} - 2c_{13}}{c_{14}(c_{13} - 1)c_S^2} \Phi^{\text{II}} N_i N_j + \delta_{ij} \Phi^{\text{II}}, \quad (2.11)$$

and  $\phi_{ij}$ ,  $\Psi^I_i$  and  $\Phi^{\text{II}}$  are, respectively, the gauge-invariant quantities of the tensor, vector and scalar modes defined in [19]. The quantities  $c_V$  and  $c_S$  denote the speeds of the vector and scalar modes, respectively. Due to their presence, the polarizations of a GW have five independent

modes which are given respectively by [19]

$$h_+^{\text{ae}} \equiv \frac{1}{2} (\mathcal{P}_{XX} - \mathcal{P}_{YY}) = \frac{G_{\text{ae}}}{R} \ddot{Q}_{kl} e_+^{kl}, \quad (2.12)$$

$$h_\times^{\text{ae}} \equiv \frac{1}{2} (\mathcal{P}_{XY} + \mathcal{P}_{YX}) = \frac{G_{\text{ae}}}{R} \ddot{Q}_{kl} e_\times^{kl}, \quad (2.13)$$

$$h_b^{\text{ae}} \equiv \frac{1}{2} (\mathcal{P}_{XX} + \mathcal{P}_{YY}) = \frac{c_{14} G_{\text{ae}}}{R(2 - c_{14})} \left[ 3(Z - 1) \ddot{Q}_{ij} e_Z^i e_Z^j - \frac{4}{c_{14} c_S} \Sigma_i e_Z^i + Z \ddot{I} \right], \quad (2.14)$$

$$h_L^{\text{ae}} \equiv \mathcal{P}_{ZZ} = \left[ 1 - \frac{c_{14} - 2c_{13}}{c_{14}(c_{13} - 1)c_S^2} \right] h_b^{\text{ae}}, \quad (2.15)$$

$$h_X^{\text{ae}} \equiv \frac{1}{2} (\mathcal{P}_{XZ} + \mathcal{P}_{ZX}) = \frac{2c_{13} G_{\text{ae}}}{(2c_1 - c_{13} c_-) c_V R} \times \left[ \frac{c_{13} \ddot{Q}_{jk} e_Z^k}{(1 - c_{13}) c_V} - 2\Sigma_j \right] e_X^j, \quad (2.16)$$

$$h_Y^{\text{ae}} \equiv \frac{1}{2} (\mathcal{P}_{YZ} + \mathcal{P}_{ZY}) = \frac{2c_{13} G_{\text{ae}}}{(2c_1 - c_{13} c_-) c_V R} \times \left[ \frac{c_{13} \ddot{Q}_{jk} e_Z^k}{(1 - c_{13}) c_V} - 2\Sigma_j \right] e_Y^j, \quad (2.17)$$

where  $c_- \equiv c_1 - c_3$ ,  $G_{\text{ae}} = G_N(1 - c_{14}/2)$ ,  $\mathcal{P}_{XY} \equiv \mathcal{P}_{ij} e_X^i e_Y^j$ , and so on. We have also defined,

$$Q_{ij} = I_{ij} - \frac{1}{3} \delta_{ij} I, \quad (2.18)$$

$$I_{ij} = \sum_a m_a x_a^i x_a^j,$$

where  $x_a^i$  is the location of the  $a$ -th body and  $I \equiv I_{kk}$ . For more details, see [19]. From the above expressions, we can see that the longitudinal mode  $h_L$  is proportional to the breathing mode  $h_b$ . Besides,  $h_X$  and  $h_Y$  modes are suppressed by the factor  $c_{13}$ , which is  $c_{13} \lesssim 10^{-15}$ . In this paper, we shall choose the four coupling constants  $c_i$ 's as,

$$c_1 = 4 \times 10^{-5}, \quad c_2 = 9 \times 10^{-5}, \quad (2.19)$$

$$c_3 = -c_1, \quad c_4 = -2 \times 10^{-5},$$

which satisfy all the theoretical and observational constraints given by Eq.(A.11) (See also the [27]). Note that for this choice we have  $c_{13} = 0$ , and then the two modes  $h_X^{\text{ae}}$  and  $h_Y^{\text{ae}}$  vanish identically,

$$h_X^{\text{ae}} = h_Y^{\text{ae}} = 0, \quad (c_{13} = 0). \quad (2.20)$$

So, in the rest of this paper, we shall not consider them any further.

In Figs. 2 and 3, we plot the two polarization modes  $h_+^{\text{ae}}$  and  $h_\times^{\text{ae}}$ , while in Figs. 4 and 5, we plot their Fourier transforms. From these figures, it can be seen clearly that

these two modes are almost identical to the ones given in GR, after all the constraints of  $\mathfrak{a}$ -theory are taken into account.

However, in addition to these two modes,  $\mathfrak{a}$ -theory predicts three more independent modes,  $h_b^{\mathfrak{a}}$ ,  $h_{\times}^{\mathfrak{a}}$  and  $h_{\vee}^{\mathfrak{a}}$ . Nevertheless, comparing to the two modes,  $h_+^{\mathfrak{a}}$  and  $h_{\times}^{\mathfrak{a}}$ , they are suppressed, respectively, by a factor,  $c_{14} \lesssim 10^{-5}$  and  $c_{13} \lesssim 10^{-15}$  [19], as can be seen from Eq.(2.12). In Fig. 6, we plot  $h_b^{\mathfrak{a}}$  and  $h_L^{\mathfrak{a}}$ , which are about three orders lower than  $h_+^{\mathfrak{a}}$  and  $h_{\times}^{\mathfrak{a}}$ .

The Fourier transform for the  $h_b$  mode is shown in Fig. 7. It is remarkable that now the two peaked frequencies are only about one time as large as the ones of the orbital frequencies for the outer and inner binaries,

$$\begin{aligned} f_{\text{outer}}^{(b,L,\mathfrak{a})} &\simeq 0.0457771 \mu\text{Hz} \simeq 1.29435 \times f_{\text{outer}}^{\text{orb}}, \\ f_{\text{inner}}^{(b,L,\mathfrak{a})} &\simeq 7.09545 \mu\text{Hz} \simeq 0.998899 \times f_{\text{inner}}^{\text{orb}}, \end{aligned} \quad (2.21)$$

where the outer and inner orbital frequencies  $f_{\text{inner}}^{\text{orb}}$  and  $f_{\text{outer}}^{\text{orb}}$  of the triple system are given by Eq.(2.9). Thus, these frequencies are about equal to  $f_{\text{inner}}^{\text{orb}}$  and  $f_{\text{outer}}^{\text{orb}}$ , but not exactly.

Note that, recently, we studied binary systems in  $\mathfrak{a}$ -theory and found that the polarization modes  $h_b$  and  $h_L$  all contain two frequency modes, one is equal to their orbital frequency and one is twice of their orbital frequency [20]. Again, the reason that  $f_{\text{outer}}^{(b,L,\mathfrak{a})}$  and  $f_{\text{inner}}^{(b,L,\mathfrak{a})}$  are not exactly equal to the outer and inner orbital frequencies  $f_{\text{inner}}^{\text{orb}}$  and  $f_{\text{outer}}^{\text{orb}}$  of the triple system is due to the influence of the third component of the triple system, rather than the predictions of the theory itself.

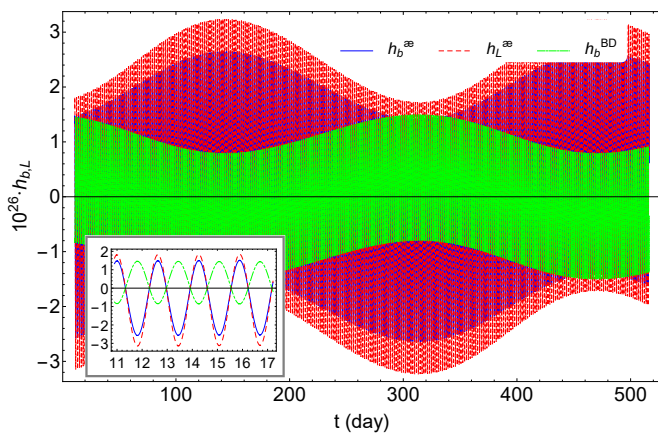


FIG. 6: The breathing ( $h_b$ ) and longitudinal ( $h_L$ ) polarization modes, respectively, in  $\mathfrak{a}$ -theory and BD gravity for about 500 days with an inserted plot for about 7 days. Note that the amplitudes are amplified by a factor  $10^{26}$ .

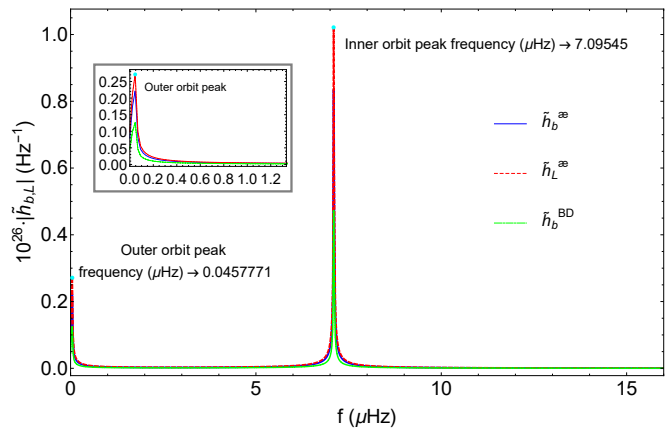


FIG. 7: The Fourier transforms of the breathing and longitudinal polarization modes in, respectively,  $\mathfrak{a}$ -theory and BD gravity, in which the peak frequencies have been marked. Note that the amplitudes are amplified by a factor  $10^{26}$ .

### C. Gravitational Waveforms and Their Polarizations in BD Gravity

The metric perturbation and scalar field perturbation are given by [21],

$$\begin{aligned} \theta^{ij} &= \frac{2}{\phi_0} \frac{1}{R} \frac{d^2}{dt^2} \sum_{a=1}^3 m_a x_a^i x_a^j, \\ \varphi^{BD} &= \frac{4}{R} (N_i \dot{M}_1^i + \frac{1}{2} N_i N_j \ddot{M}_2^{ij}), \end{aligned} \quad (2.22)$$

where  $\phi_0$  is the value of the BD field in the Minkowski background, which satisfies  $\phi_0 = (4 + 2\omega_{BD}) / [(3 + 2\omega_{BD})G_N]$  [22], and

$$\begin{aligned} M_1^i &= \frac{1}{6+4\omega_{BD}} \sum_{a=1}^3 m_a (1 - 2s_a) x_a^i, \\ M_2^{ij} &= \frac{1}{6+4\omega_{BD}} \sum_{a=1}^3 m_a (1 - 2s_a) x_a^i x_a^j, \end{aligned} \quad (2.23)$$

where  $\omega_{BD}$  is the BD parameter of the theory. In this paper, we choose sensitivities such that  $s_1$  (for pulsar) = 0.2,  $s_2$  (for inner WD) = 0,  $s_3$  (for outer WD) = 0 and the coupling constant  $\omega_{BD} = 10^5$  [13]. Note that in writing the above expressions, we had dropped the non-propagating terms in  $\varphi^{BD}$ . Then, the components  $R_{0i0j}$  of the Riemann tensor can be cast in the form,

$$R_{0i0j} = -\frac{1}{2} \frac{d^2}{dt^2} \left[ \theta_{ij}^{TT} - \frac{\varphi^{BD}}{\phi_0} (\delta_{ij} - N_i N_j) \right]. \quad (2.24)$$

Then, it can be shown that there are only three independent polarization modes, given, respectively, by

$$\begin{aligned} h_+^{BD} &= \frac{1}{2} e_+^{ij} \theta_{ij}, \quad h_{\times}^{BD} = \frac{1}{2} e_{\times}^{ij} \theta_{ij}, \\ h_b^{BD} &= -\frac{\varphi^{BD}}{\phi_0}, \end{aligned} \quad (2.25)$$

which are plotted out, respectively, in Figs. 2, 3 and 6, while their Fourier transforms are plotted out in Figs. 4, 5 and 7. From these figures, it can be seen that the amplitudes of the two polarization modes  $h_+^{BD}$  and  $h_\times^{BD}$  are in the same order as those in GR and  $\mathfrak{a}$ -theory, due to the observational constraints on the  $\omega_{BD}$ .

However, the amplitude of the breathing mode  $h_b^{BD}$  is smaller than  $h_b^{\mathfrak{a}}$ , as can be seen from Fig. 6. But, somehow it is surprising that its Fourier transform has also two peaked frequencies and are equal to these of  $h_b^{\mathfrak{a}}$  and  $h_L^{\mathfrak{a}}$ ,

$$\begin{aligned} f_{\text{outer}}^{(b, \text{BD})} &\simeq f_{\text{outer}}^{(b, L, \mathfrak{a})} \simeq 0.0457771 \mu\text{Hz}, \\ f_{\text{inner}}^{(b, \text{BD})} &\simeq f_{\text{inner}}^{(b, L, \mathfrak{a})} \simeq 7.09545 \mu\text{Hz}. \end{aligned} \quad (2.26)$$

Thus, in contrast to the polarization modes  $h_+$  and  $h_\times$ , which also have two peaked frequencies, but are about twice of those of the outer and inner orbital frequencies.

### III. RADIATION POWERS

In GR, the total radiation power is given by [17, 23],

$$P^{GR} = \frac{G_N}{5} \langle \ddot{Q}_{ij} \ddot{Q}_{ij} \rangle, \quad (3.1)$$

where  $Q_{ij}$  is the mass quadrupole moment defined in Eq.(2.18) and the angular brackets denote the time average as in [25]<sup>1</sup>. Note that in this section we shall not distinguish the time  $t$  and its corresponding retarded time. Strictly speaking, all the quantities should be evaluated at the retarded time. However, it is not necessary for our current purpose.

The reference frame is chosen such that the inclination is  $39.25^\circ$ , where the inclination is the angle of the plane of the orbit relative to the  $(x, y)$ -plane perpendicular to the line-of-sight from Earth to the pulsar. In Fig. 8, we plot the radiation power in GR for about 500 days, where the inserted smaller image shows the details from day 11 to day 21.

In  $\mathfrak{a}$ -theory, from [19, 24] we find that

$$P^{\mathfrak{a}} = G_N \left\langle \frac{\mathcal{A}}{5} \ddot{Q}_{ij} \ddot{Q}_{ij} + \mathcal{B} \ddot{I} \ddot{I} + \mathcal{C} \dot{\Sigma}_i \dot{\Sigma}_i \right\rangle, \quad (3.2)$$

where  $\Sigma_i$  is defined as

$$\Sigma_i = (\alpha_1 - \frac{2}{3}\alpha_2) \sum_a (v_a^i \Omega_a), \quad (3.3)$$

<sup>1</sup> However, since we are considering periodic GWs, we will not take this time average in the relevant plots. Otherwise, it will be zero for such periodic waves. The same will also apply to the cases of  $\mathfrak{a}$ -theory and BD gravity.

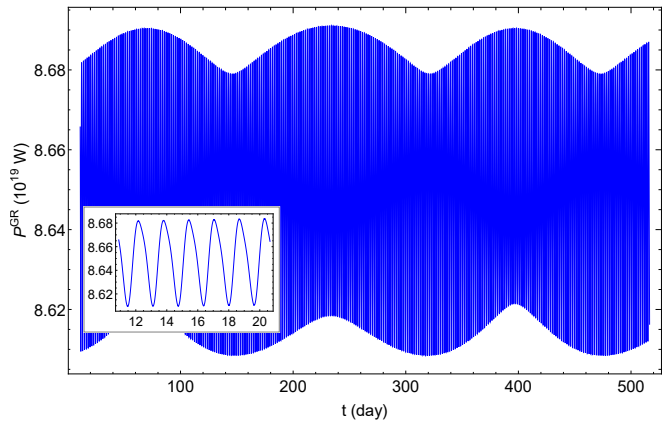


FIG. 8: The instantaneous (time un-averaged) radiation power in GR for about 500 days with an inserted plot for about 10 days. Note that the unit of the power in this plot is  $10^{19}$  Watt.

and

$$\begin{aligned} \mathcal{A} &\equiv \left(1 - \frac{c_{14}}{2}\right) \left( \frac{1}{c_T} + \frac{2c_{14}c_{13}^2}{(2c_1 - c_{13}c_-)^2 c_V} \right. \\ &\quad \left. + \frac{3(Z-1)^2 c_{14}}{2(2-c_{14})c_S} \right), \\ \mathcal{B} &= \frac{Z^2 c_{14}}{8c_S}, \\ \mathcal{C} &\equiv \frac{2}{3c_{14}} \left( \frac{2-c_{14}}{c_V^3} + \frac{1}{c_S^3} \right), \\ Z &\equiv \frac{(\alpha_1 - 2\alpha_2)(1 - c_{13})}{3(2c_{13} - c_{14})}, \end{aligned} \quad (3.4)$$

with [25],

$$\begin{aligned} \alpha_1 &= -\frac{8(c_1 c_{14} - c_- c_{13})}{2c_1 - c_- c_{13}}, \\ \alpha_2 &= \frac{1}{2}\alpha_1 + \frac{(c_{14} - 2c_{13})(3c_2 + c_{13} + c_{14})}{c_{123}(2 - c_{14})}. \end{aligned} \quad (3.5)$$

Here  $v_a^i \equiv \dot{x}_a^i$  is the velocity of  $a$ -th body along  $x^i$ -direction,  $\Omega_a$  is the binding energy of  $a$ -th body. For J0337 [11], we have  $\Omega_1$  (for pulsar)  $= -2.56955 \times 10^{46}$  J,  $\Omega_2$  (for inner WD)  $= -9.75554 \times 10^{40}$  J,  $\Omega_3$  (for outer WD)  $= -2.12650 \times 10^{42}$  J. where  $c_T$ ,  $c_V$  and  $c_S$  are the speeds of the tensor, vector and scalar modes, given by Eq.(A.7) in Appendix A, in which the definitions  $c_{ijk} \equiv c_i + c_j + c_k$  and  $c_{ij} \equiv c_i + c_j$  are given.

In Fig. 9, we plot the radiation power in  $\mathfrak{a}$ -theory of the parts  $\mathcal{A}$ ,  $\mathcal{B}$  and  $\mathcal{C}$  separately, for about 500 days. Again, the inserted smaller images are from day 11 to day 21. Note that at every moment during the 500 days in the plot, the  $\mathcal{A}$  part of  $\mathfrak{a}$ -theory is quite close to that of GR with the difference proportional to  $c_{14}$  [19],

$$\frac{P_{\mathcal{A}}^{\mathfrak{a}}}{P_{\mathcal{A}}^{GR}} \simeq 1 + \mathcal{O}(c_{14}) \lesssim \mathcal{O}(10^{-5}). \quad (3.6)$$

From this figure, it is also clear that the dipole part  $\mathcal{C}$  has almost the same amplitude as that of the quadrupole part  $\mathcal{A}$ , while the monopole part  $\mathcal{B}$  is suppressed by a factor  $c_{14}$ , as now we have  $\alpha_i \simeq \mathcal{O}(c_{14})$ ,  $Z \simeq \mathcal{O}(1)$  [19]. The large magnitude of the dipole contribution  $\mathcal{C}$  seemingly contradicts to the analysis given in [19]. In particular, Eq.(3.13) in [19] shows that  $\mathcal{W}_C^{\text{NS}}/\mathcal{W}_A^{\text{NS}} \simeq 10^{-2}$ , where

$$\begin{aligned} \mathcal{W}_A &\equiv \frac{8}{15} \mathcal{A} (12v^2 - 11r^2), \\ \mathcal{W}_C &\equiv \mathcal{C} \Sigma^2, \end{aligned} \quad (3.7)$$

where  $\mathcal{A}$ ,  $\mathcal{C}$  and  $\Sigma$  are all given explicitly in [19]. However, in deriving Eq.(3.6) we assumed that  $\mathcal{O}(v^2) \simeq 10^{-5}$ , while in the current case we find that the relative velocities of the inner binary system are of the order of  $\mathcal{O}(v^2) \simeq 10^{-7}$ . After this is taken into account, we find that  $\mathcal{W}_C^{\text{NS}}/\mathcal{W}_A^{\text{NS}} \simeq \mathcal{O}(1)$  for the current triple system.

It is remarkable to note that, with the multi-band gravitational wave astronomy [16], joint observations of GW150914-like by LIGO/Virgo/KAGRA and LISA will improve bounds on dipole emission from black hole binaries by six orders of magnitude relative to current constraints [26]. Thus, it is very promising that the third generation of detectors, both space-borne and ground-based, could provide severe constraints on  $\mathfrak{a}$ -theory.

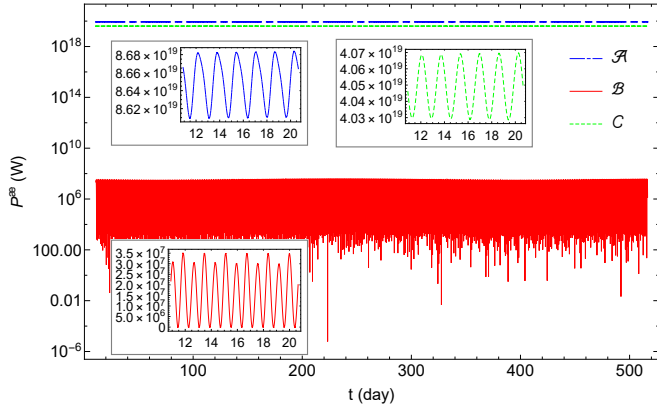


FIG. 9: The instantaneous (time un-averaged) radiation power in  $\mathfrak{a}$ -theory. Here the  $\mathcal{A}$ ,  $\mathcal{B}$  and  $\mathcal{C}$  parts are plotted separately.

In BD gravity, following [21] we obtain

$$P^{BD} = P_1^{BD} + P_2^{BD}, \quad (3.8)$$

where

$$\begin{aligned} P_1^{BD} &= \frac{1}{\phi_0} \left\langle \frac{1}{5} \ddot{Q}_{ij} \ddot{Q}_{ij} \right\rangle, \\ P_2^{BD} &= \frac{1}{\phi_0} \left\langle \frac{2\omega + 3}{\pi} \left[ \frac{4\pi}{3} \ddot{M}_1^i \ddot{M}_1^i \right. \right. \\ &\quad \left. \left. + \frac{\pi}{12} \left( \ddot{M}_2^{ii} \ddot{M}_2^{jj} + 2\ddot{M}_2^{ij} \ddot{M}_2^{ij} \right) \right] \right\rangle, \end{aligned} \quad (3.9)$$

where  $M_1^i$  and  $M_2^{ij}$  are defined by Eq.(2.23). Note that in writing down the above expressions, we had dropped the non-propagating terms.

In Fig. 10, we plot the radiation power in BD gravity for about 500 days, where the inserted smaller image shows the details only for 10 days (from day 11 to day 21). Note that at every moment during the 500 days, the first part of BD is quite close to that given in GR. In fact, we find that

$$\frac{P_1^{BD}}{P_{GR}} \simeq 1 + \mathcal{O}(\omega_{BD}^{-1}) \lesssim \mathcal{O}(10^{-5}). \quad (3.10)$$

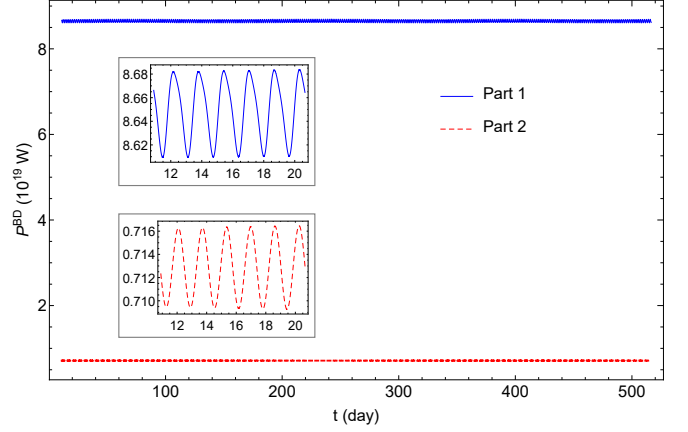


FIG. 10: The instantaneous (time un-averaged) radiation power in BD gravity. Here the part 1 and 2 are plotted, separately. Note that the unit of the power in this plot is  $10^{19}$  Watt.

## IV. CONCLUSIONS

In this paper, we studied the gravitational waveforms, their polarizations and Fourier transforms, as well as the radiation powers of the relativistic triple systems PSR J0337 + 1715, observed in 2014 [11]. This system consists of an inner binary and a third companion. The inner binary consists of a pulsar with mass  $m_1 = 1.44M_\odot$  and a white dwarf with mass  $m_2 = 0.20M_\odot$  in a 1.6 day orbit. The outer binary consists of the inner binary and a second dwarf with mass  $m_3 = 0.41M_\odot$  in a 327 day orbit. The two orbits are very circular with its eccentricities  $e_I \simeq 6.9 \times 10^{-4}$  for the inner binary and  $e_O \simeq 3.5 \times 10^{-2}$  for the outer orbit. The two orbital planes are remarkably coplanar with an inclination  $\lesssim 0.01^\circ$  [See Fig. 1].

Our studies were carried out in three different theories, GR, BD gravity, and  $\mathfrak{a}$ -theory. In GR, only the tensor mode exists, so a GW has only two polarization modes, the so-called, plus ( $h_+$ ) and cross ( $h_\times$ ) modes. Their amplitudes and Fourier transforms are plotted in Figs. 2 - 4, from which it can be seen that their amplitude is about  $10^{-23}$ , while their frequencies are peaked in two locations,  $f_1^{(+,\times)} = 0.0686656\mu\text{Hz}$  (for the outer orbit) and

$f_2^{(+,\times)} = 14.2138\mu\text{Hz}$  (for the inner orbit), respectively. These are about two times of the inner and outer orbital frequencies of the triple system, and agree well with the GR predictions [17].

In  $\text{\ae}$ -theory, all the six polarization modes are different from zero, but the beating ( $h_b$ ) and longitudinal ( $h_L$ ) modes are not independent and are related to each other by Eq.(2.12). In comparing with  $h_+$  and  $h_\times$ , however, they are suppressed by a factor  $c_{14}$  which is observationally restricted to  $c_{14} \lesssim 10^{-5}$  [27]. A somehow surprising result is that the two peaked frequencies are not two times of those of the inner and outer orbital frequencies of the triple system. Instead, they are about equal to them,  $f_1^{(b,L)} = 0.0457771\mu\text{Hz}$  (for the outer orbit) and  $f_2^{(b,L)} = 7.09545\mu\text{Hz}$  (for the inner orbit) [Cf. Fig. 7].

The other two independent polarization modes in  $\text{\ae}$ -theory are the vector modes,  $h_X$  and  $h_Y$ , which are all proportional to  $c_{13}$ . The current observations from GW170817 [7] and GRB 170817A [28] on the speed of the tensor mode requires  $c_{13} \lesssim 10^{-15}$ . Therefore, these two modes are highly restricted by the limit of the speed of the tensor mode.

We also studied the radiation power due to the tensor, vector and scalar modes in  $\text{\ae}$ -theory, and three different parts were plotted in Fig. 9. The amplitude of the quadrupole part ( $\mathcal{A}$ ), contributed from all of these three modes, tensor, vector and scalar [19, 24] is quite comparable with that of GR. But, the monopole ( $\mathcal{B}$ ) part has contributions only from the scalar mode, while the dipole ( $\mathcal{C}$ ) part has contributions from both the scalar and vector modes, but does not have any contributions from the tensor mode, as expected [19, 24]. The monopole part is suppressed by a factor  $c_{14} \lesssim \mathcal{O}(10^{-5})$ , but the dipole part is almost in the same order of the quadrupole part. With the arrival of the multi-band gravitational wave astronomy [16], joint observations of GW150914-like by LIGO/Virgo/KAGRA and LISA will improve serve constraints on the dipole emission [26]. Thus, the multi-band gravitational wave astronomy will provide a very promising direction to constrain  $\text{\ae}$ -theory.

We also carried out similar studies in BD gravity, and the relevant quantities were plotted in Figs. 2 - 7 and 10. Due to the severe observational constraint on the BD parameter  $\omega_{BD} \gtrsim 10^5$ , we did not find significant deviations from GR, except that the frequency of the breathing mode  $h_b$  is also peaked in two locations,  $f_1^b \simeq f_1^{(b,L)} = 0.0457771\mu\text{Hz}$  and  $f_2^b \simeq f_2^{(b,L)} = 7.09545\mu\text{Hz}$ , which are about equal to those of the inner and outer orbital frequencies of the triple system, quite similar to that in  $\text{\ae}$ -theory [Cf. Fig. 7] but with a low amplitude.

### Acknowledgments

We would like to thank Dr. Lijing Shao for providing us the original data of PSR J0337+1715. This work is supported in part by the National Natural

Foundation of China (NNSFC) with the grant numbers: Nos. 11603020, 11633001, 11173021, 11322324, 11653002, 11421303, 11375153, 11675145, 11675143, 11105120, 11805166, 11835009, 11690022, 11375247, 11435006, 11575109, 11647601, and No. 11773028.

### Appendix A: Einstein-aether Theory

In this appendix, we shall give a brief introduction to Einstein-aether Theory. For detail, we refer readers to Jacobson's review [14], and [19] for recent development. In  $\text{\ae}$ -theory, the fundamental variables are [29],

$$(g_{\mu\nu}, u^\mu, \lambda), \quad (\text{A.1})$$

where  $g_{\mu\nu}$  is the four-dimensional metric of the space-time,  $u^\mu$  is the aether four-velocity, and  $\lambda$  is a Lagrangian multiplier, which guarantees that the aether four-velocity is always timelike. The general action of  $\text{\ae}$ -theory is given by [14],

$$S = S_{\text{\ae}} + S_m, \quad (\text{A.2})$$

where  $S_m$  denotes the action of matter, and  $S_{\text{\ae}}$  the gravitational action of the  $\text{\ae}$ -theory, given by

$$\begin{aligned} S_{\text{\ae}} &= \frac{1}{16\pi G_{\text{\ae}}} \int \sqrt{-g} d^4x \left[ R(g_{\mu\nu}) + \mathcal{L}_{\text{\ae}}(g_{\mu\nu}, u^\alpha, \lambda) \right], \\ S_m &= \int \sqrt{-g} d^4x \left[ \mathcal{L}_m(g_{\mu\nu}, u^\alpha; \psi) \right]. \end{aligned} \quad (\text{A.3})$$

Here  $\psi$  collectively denotes the matter fields,  $R$  and  $g$  are, respectively, the Ricci scalar <sup>2</sup> and determinant of  $g_{\mu\nu}$ , and

$$\mathcal{L}_{\text{\ae}} \equiv -M^{\alpha\beta}{}_{\mu\nu} (D_\alpha u^\mu) (D_\beta u^\nu) + \lambda (g_{\alpha\beta} u^\alpha u^\beta + 1), \quad (\text{A.4})$$

where  $D_\mu$  denotes the covariant derivative with respect to  $g_{\mu\nu}$ , and  $M^{\alpha\beta}{}_{\mu\nu}$  is defined as

$$M^{\alpha\beta}{}_{\mu\nu} \equiv c_1 g^{\alpha\beta} g_{\mu\nu} + c_2 \delta_\mu^\alpha \delta_\nu^\beta + c_3 \delta_\nu^\alpha \delta_\mu^\beta - c_4 u^\alpha u^\beta g_{\mu\nu}. \quad (\text{A.5})$$

The four coupling constants  $c_i$ 's are all dimensionless, and  $G_{\text{\ae}}$  is related to the Newtonian constant  $G_N$  via the relation [30],

$$G_N = \frac{G_{\text{\ae}}}{1 - \frac{1}{2}c_{14}}, \quad (\text{A.6})$$

where  $c_{ij} \equiv c_i + c_j$ .

It is easy to show that the Minkowski spacetime is a solution of  $\text{\ae}$ -theory, in which the aether is aligned

<sup>2</sup> Note that  $R$  here is different from the one used in Sec.II.A which denotes the distance.



along the time direction,  $\bar{u}_\mu = \delta_\mu^0$ . Then, the linear perturbations around the Minkowski background show that the theory in general possess three types of excitations, scalar, vector and tensor modes [31], with their squared speeds given, respectively, by

$$\begin{aligned} c_S^2 &= \frac{c_{123}(2 - c_{14})}{c_{14}(1 - c_{13})(2 + c_{13} + 3c_2)}, \\ c_V^2 &= \frac{2c_1 - c_{13}(2c_1 - c_{13})}{2c_{14}(1 - c_{13})}, \\ c_T^2 &= \frac{1}{1 - c_{13}}, \end{aligned} \quad (\text{A.7})$$

where  $c_{ijk} \equiv c_i + c_j + c_k$ .

Recently, the combination of the gravitational wave event GW170817 [7], and the event of the gamma-ray burst GRB 170817A [28] provides a remarkably stringent constraint on the speed of the spin-2 mode,

$$-3 \times 10^{-15} < c_T - 1 < 7 \times 10^{-16}, \quad (\text{A.8})$$

which, together with Eq.(A.7), implies that

$$|c_{13}| < 10^{-15}. \quad (\text{A.9})$$

Imposing further the following conditions: (a) the theory is free of ghosts; (b) the squared speeds  $c_I^2$  ( $I = S, V, T$ ) must be non-negative; (c)  $c_T^2 - 1$  must be greater than  $-10^{-15}$  or so, in order to avoid the existence of the vacuum gravi-Čerenkov radiation by matter such as cosmic rays [32]; and (d) the theory must be consistent with the current observations on the primordial helium abundance  $|G_{cos}/G_N - 1| \lesssim 1/8$ , where  $G_{cos} \equiv G_{\text{ae}}/(1 + (c_{13} + 3c_2)/2)$  [30], together with Eq.(A.9) and the conditions,

$$|\alpha_1| \leq 10^{-4}, \quad |\alpha_2| \leq 10^{-7}, \quad (\text{A.10})$$

from the Solar System observations [33], it was found that the parameter space of the theory is restricted to [27],

$$0 \lesssim c_{14} \lesssim c_1, \quad c_{14} \lesssim c_2 \lesssim 0.095, \quad c_{14} \lesssim 2.5 \times 10^{-5}. \quad (\text{A.11})$$

Finally, we note that the theoretical and observational constraints of  $\text{ae}$ -theory and gravitational waves were also studied in [34].

- 
- [1] E. Schucking *et al.*, The Collected Papers of Albert Einstein vol6, The Berlin Years, Princeton University Press, Princeton, New Jersey, ISBN: 0-691-01734-4 (1997).
- [2] B.P. Abbott, *et al.*, [LIGO Scientific and Virgo Collaborations] Phys. Rev. Lett. **116**, 061102 (2016).
- [3] B.P. Abbott, *et al.*, [LIGO Scientific and Virgo Collaborations] Phys. Rev. Lett. **116**, 241103 (2016).
- [4] B.P. Abbott, *et al.*, [LIGO Scientific and Virgo Collaborations] Phys. Rev. Lett. **118**, 221101 (2017).
- [5] B.P. Abbott, *et al.*, [LIGO Scientific and Virgo Collaborations] Astrophys. J. **851**, L35 (2017).
- [6] B.P. Abbott, *et al.*, [LIGO Scientific and Virgo Collaborations] Phys. Rev. Lett. **119**, 141101 (2017).
- [7] B.P. Abbott, *et al.*, [LIGO Scientific and Virgo Collaborations] Phys. Rev. Lett. **119**, 161101 (2017).
- [8] B.P. Abbott, *et al.* [LIGO/Virgo Collaborations], arXiv:1811.12907.
- [9] K. Fuhrmann, *et al.*, Astrophys. J. **836** (2017) 139.
- [10] A. Tokovinin, *et al.*, A & A **450** (2006) 681.
- [11] S. Ransom, *et al.*, Nature **505** (2014) 520.
- [12] L. Shao, Phys. Rev. D **93**, 084023 (2016).
- [13] A. Archibald, *et al.*, Nature **559** (2018) 73.
- [14] T. Jacobson, Einstein- $\text{ae}$ ther gravity: a status report, arXiv:0801.1547.
- [15] Brans, C. H.; Dicke, R. H. (November 1, 1961). "Mach's Principle and a Relativistic Theory of Gravitation", Physical Review. 124 (3): 925, 935.
- [16] A. Sesana, Prospects for Multi-band Gravitational-Wave Astronomy after GW150914, Phys. Rev. Lett. **116**, 231102 (2016).
- [17] M. Maggiore, Gravitational Waves Volume 1: Theory and Experiments (Oxford University Press, New York, 2016).
- [18] , C. J. Moore, R. H. Cole and C. P. L. Berry, Class. Quantum Grav. **32** 015014 (2015).
- [19] K. Lin, *et al.*, Gravitational wave forms, polarizations, response functions and energy losses of triple systems in Einstein-Aether theory, arXiv:1810.07707.
- [20] X. Zhao, *et al.*, in preparation (2019).
- [21] C. M. Will, Gravitational radiation, close binary systems, and the Brans-Dicke theory of gravity, DOI: 10.1086/168016.
- [22] X. Zhang, *et al.*, Phys. Rev. Lett. **95**, 124008 (2017).
- [23] V. Dmitrasinovic, M. Suvakov, and A. Hudomal, Phys. Rev. Lett. **113**, 101102 (2014).
- [24] B. Z. Foster, Radiation Damping in Einstein-Aether Theory, arXiv:gr-qc/0602004v5.
- [25] B. Z. Foster, Post-Newtonian parameters and constraints on Einstein-aether theory, PRD **73**, 064015 (2006).
- [26] E. Berti, K. Yagi, and N. Yunes, Extreme gravity tests with gravitational waves from compact binary coalescences: (I) inspiral-merger, Gen. Relativ. Grav. **50**, 46 (2018).
- [27] J. Oost, S. Mukohyama and A. Wang, Constraints on Einstein-aether theory after GW170817, arXiv:1802.04303.
- [28] B. P. Abbott *et al.*, Virgo, Fermi-GBM, INTEGRAL, LIGO Scientific Collaboration, Gravitational Waves and Gamma-rays from a Binary Neutron Star Merger: GW170817 and GRB 170817A, Astrophys. J. **848** (2017) L13 [arXiv:1710.05834].
- [29] T. Jacobson, D. Mattingly, Phys. Rev. D **64**, 024028 (2001).
- [30] S. M. Carroll and E. A. Lim, Phys. Rev. D **70**, 123525 (2004).
- [31] T. Jacobson, D. Mattingly, Phys. Rev. D **70**, 024003

- (2004).
- [32] J. W. Elliott, G. D. Moore and H. Stoica, JHEP **0508**, 066 (2005) [arXiv:hep-ph/0505211].
- [33] C. M. Will, Living Reviews in Relativity **9**, 3 (2006).
- [34] Y.-G. Gong, S.-Q. Hou, D.-C. Liang, E. Papantonopoulos, Phys. Rev. D**97**, 084040 (2018).